

# Host–Guest Hybrid Redox Materials Self-Assembled from Polyoxometalates and Single-Walled Carbon Nanotubes

Jack W. Jordan, Grace A. Lowe, Robert L. McSweeney, Craig T. Stoppiello, Rhys W. Lodge, Stephen T. Skowron, Johannes Biskupek, Graham A. Rance, Ute Kaiser, Darren A. Walsh,\* Graham N. Newton,\* and Andrei N. Khlobystov\*

The development of next-generation molecular-electronic, electrocatalytic, and energy-storage systems depends on the availability of robust materials in which molecular charge-storage sites and conductive hosts are in intimate contact. It is shown here that electron transfer from single-walled carbon nanotubes (SWNTs) to polyoxometalate (POM) clusters results in the spontaneous formation of host–guest POM@SWNT redox-active hybrid materials. The SWNTs can conduct charge to and from the encapsulated guest molecules, allowing electrical access to >90% of the encapsulated redox species. Furthermore, the SWNT hosts provide a physical barrier, protecting the POMs from chemical degradation during charging/discharging and facilitating efficient electron transfer throughout the composite, even in electrolytes that usually destroy POMs.

The development of advanced molecular materials for applications such as energy storage and molecular computing depends on the availability of robust, redox-active solid-state materials.<sup>[1]</sup> Polyoxometalates (POMs) are nanometer-sized clusters of early transition metal (Mo, W, V, Nb, Ta) oxides with well-defined compositions and structures and which can undergo multi-electron redox transitions,<sup>[2]</sup> rendering them promising nodes for molecular flash memory systems<sup>[3]</sup> and as the redox components in

electrochemical energy-storage devices.<sup>[4]</sup> However, two major hurdles must be overcome to realize these opportunities: i) fully oxidized POMs are electrically insulating, limiting the flow of charge to and from redox centers, and ii) POMs are often chemically and electrochemically unstable, especially in alkaline media.

Immobilization of POMs onto high-surface-area, conductive substrates such as single-walled carbon nanotubes (SWNTs) can potentially improve the electrical addressability and stability of the redox centers. This has been achieved using covalent functionalization of SWNTs,<sup>[5]</sup> electrostatic binding of POMs to SWNTs via covalently linked organic cations,<sup>[6]</sup> and

noncovalent interactions mediated by the organic “antenna” groups of functionalized POMs.<sup>[7]</sup> However, the conductivity of SWNTs is reduced by covalent modification of the sp<sup>2</sup> carbon framework and electrostatically bound POMs can be relatively easily dislodged from the carbon surface.<sup>[8]</sup> A possible strategy for increasing the stability of POMs at SWNT interfaces is to immobilize the POMs within SWNTs, potentially protecting them from detachment and/or degradation. Individual hexanuclear [W<sub>6</sub>O<sub>19</sub>]<sup>2−</sup> Lindqvist anions have been encapsulated within double-walled carbon nanotubes by nanoextraction from ethanolic solutions. However, the work did not extend to an exploration of the electrochemical properties of the hybrid materials.<sup>[9]</sup> The lack of further progress in this area may be due to the assumed incompatibility of highly charged POMs with the hydrophobic interior of SWNTs, a perception that is supported by recent predictions of strong repulsive interactions between ionic guests and the cavities of SWNTs.<sup>[10]</sup> As such, most work has focused on encapsulating charge-neutral species such as salts,<sup>[11]</sup> metallic and nonmetallic nanostructures,<sup>[12]</sup> and organic molecules,<sup>[13]</sup> within SWNTs.


Here, we report a surprisingly simple and highly efficient method for immobilizing POMs within SWNTs. Our method requires no reagents other than pristine SWNTs and aqueous POM solutions, and results in durable POM@SWNT hybrids in which the redox centers are electronically addressable, even in alkaline electrolytes that usually destroy POMs. [PW<sub>12</sub>O<sub>40</sub>]<sup>3−</sup>, {W<sub>12</sub>}, and [P<sub>2</sub>W<sub>18</sub>O<sub>62</sub>]<sup>6−</sup>, {W<sub>18</sub>}, both of which are about 1 nm wide, were encapsulated within arc-discharge SWNTs with average diameters of 1.4 nm.<sup>[14]</sup> Addition of SWNTs to aqueous solutions of {W<sub>12</sub>} and {W<sub>18</sub>} results in

J. W. Jordan, Dr. R. L. McSweeney, Dr. C. T. Stoppiello, Dr. R. W. Lodge, Dr. S. T. Skowron, Prof. A. N. Khlobystov  
School of Chemistry  
University of Nottingham  
Nottingham NG7 2RD, UK  
E-mail: andrei.khlobystov@nottingham.ac.uk

G. A. Lowe, Dr. D. A. Walsh, Dr. G. N. Newton  
GSK Carbon Neutral Laboratories for Sustainable Chemistry  
University of Nottingham  
Nottingham NG7 2TU, UK  
E-mail: darren.walsh@nottingham.ac.uk;  
graham.newton@nottingham.ac.uk

Dr. J. Biskupek, Prof. U. Kaiser  
Electron Microscopy Group of Materials Science  
Ulm University  
89081 Ulm, Germany

Dr. G. A. Rance  
Nanoscale and Microscale Research Centre  
University of Nottingham  
Nottingham NG7 2RD, UK

 The ORCID identification number(s) for the author(s) of this article can be found under <https://doi.org/10.1002/adma.201904182>.

DOI: 10.1002/adma.201904182

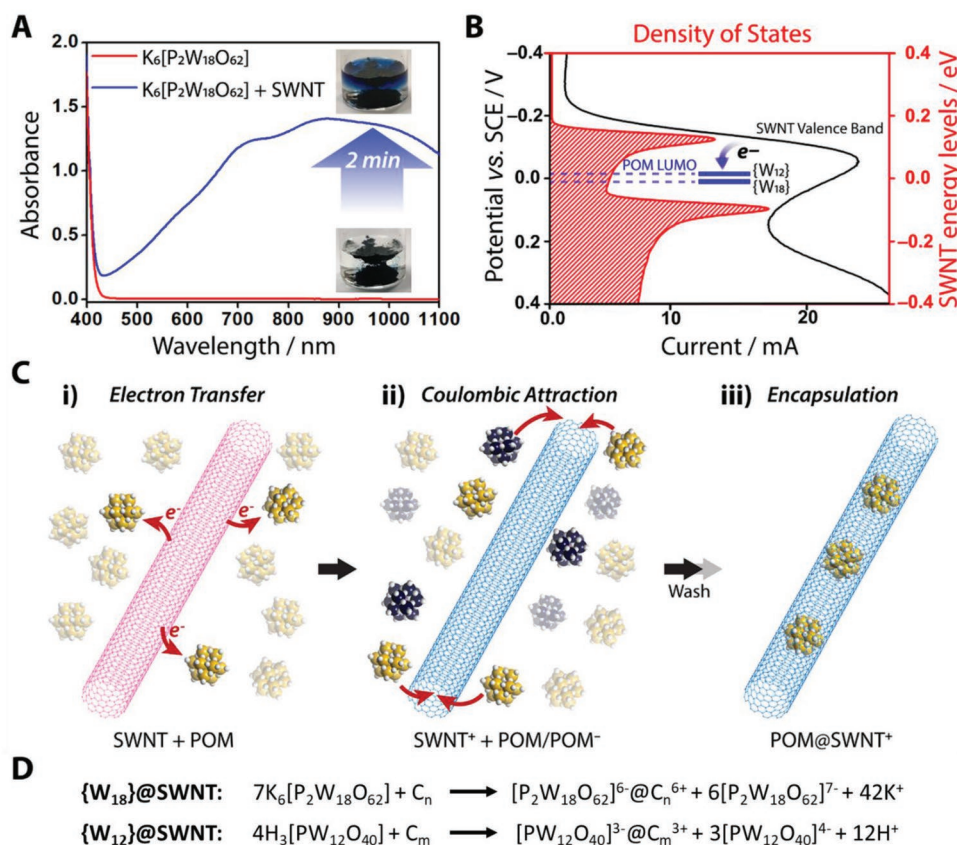


**Figure 1.** A) UV-vis absorption spectrum of an aqueous solution of  $K_6[P_2W_{18}O_{62}]$  before (red) and after contact with SWNTs (blue). B) Electronic states of a (17,0) carbon nanotube (red plot), LUMO energy of POMs (blue, taken from CV in Figure 3B,C) and linear sweep voltammogram (LSV) of open, empty SWNTs (black plot). C) Diagram showing: i) electron transfer from SWNTs (pink—neutral, blue—cationic) to POMs (yellow—native state, dark blue—reduced state); ii) Coulombic force-driven encapsulation of POM anions into the cationic SWNTs; iii) nonencapsulated POM anions and all potassium cations are washed away using water. D) Balanced equations of the redox reactions between POMs and nanotubes leading to POM encapsulation based on integration of TEM, Raman, EDX, TGA, and XPS analytical data, where  $n = 420$  and  $m = 530$  are the estimated numbers of carbon atoms of the nanotube per encapsulated POM molecule.

reduction of the POMs, as indicated by the dark blue coloration of the solution (Figure 1A) at the solid-liquid interface (reminiscent of the formation of “heteropoly blues”).<sup>[15]</sup> A similar type of electron transfer from SWNTs to metal-polyiodide clusters has been demonstrated to stabilize electron-accepting molecules in SWNTs.<sup>[16]</sup> Electron density is transferred from the SWNTs to the POMs, resulting in the electrostatically driven encapsulation of the negatively charged POMs within the now positively charged SWNTs. (Figure 1B,C) The close fit between the crystallographic dimensions of the POMs and the internal diameter of the SWNTs indicates that the POMs desolvate upon entry, providing an additional entropic driving force for encapsulation. Linear sweep voltammetry (LSV) of empty SWNTs shows that low currents flow at voltages corresponding to the energy of the SWNT bandgap, and high currents flow at voltages corresponding to the energies of the van Hove singularities.<sup>[17]</sup> The Fermi potential of the SWNTs (top level of the highest van Hove singularity in the valence band) is higher than those of the POM lowest unoccupied molecular orbitals (LUMOs) (estimated from solution-phase voltammetry of the POMs, Figure 3B,C), explaining the spontaneous electron transfer from the SWNTs to POMs (Figure 1B).<sup>[18]</sup>

High-resolution transmission electron microscopy (HRTEM) of the POM@SWNT hybrid confirms that virtually all SWNTs are filled with POMs (Figure 2J). Note that HRTEM exposure times were kept to a minimum to avoid sample degradation (Figures S1 and S2, Supporting Information). The dark-contrast POMs in the TEM images are 1.0–1.8 nm wide, indicating that the POMs have different orientations within the SWNT cavities (Figure 2E,F), similar to their behavior on graphene.<sup>[19]</sup> Aberration-corrected HRTEM (AC-HRTEM) imaging of individual molecules shows W–W distances between 2.5 and 3 Å, and energy-dispersive X-ray (EDX) analysis gives W:O ratios of 1:4.3 and 1:3.6, for  $\{W_{12}\}@SWNT$  and  $\{W_{18}\}@SWNT$ , respectively. No significant potassium signal was observed, indicating that potassium remained in solution during the nanotube-filling process (Figure 2G,H).

Thermogravimetric analysis (TGA) reveals that the average loadings of the POMs in the SWNTs are 11–16 and 11–30 wt% for  $\{W_{12}\}@SWNT$  and  $\{W_{18}\}@SWNT$ , respectively (Figure S3, Supporting Information), consistent with the HRTEM data (Figure 2J). The charge distribution within the hybrid materials was elucidated by Raman spectroscopy using an excitation wavelength of 660 nm (1.88 eV), in resonance with the SWNTs.<sup>[16]</sup>

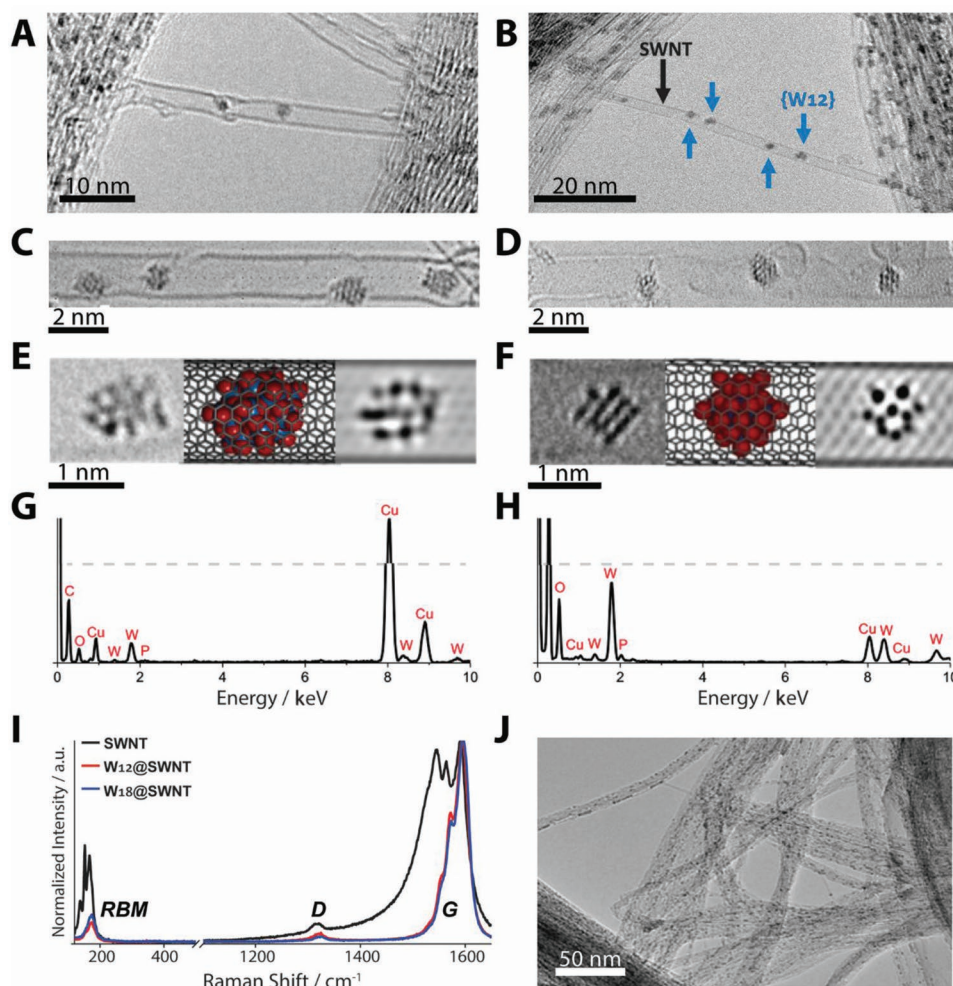


**Figure 2.** A,B) HRTEM images of {W<sub>18</sub>}@SWNT and {W<sub>12</sub>}@SWNT, respectively; C,D) AC-HRTEM images of {W<sub>18</sub>}@SWNT and {W<sub>12</sub>}@SWNT; E,F) Experimental TEM images, molecular models, and simulated images of single {W<sub>18</sub>} and {W<sub>12</sub>} POMs, respectively, in SWNTs. G,H) EDX spectra of {W<sub>18</sub>}@SWNT and {W<sub>12</sub>}@SWNT, respectively. I) Raman spectra of SWNTs, {W<sub>18</sub>}@SWNT, and {W<sub>12</sub>}@SWNT, showing the radial-breathing mode (RBM), D, and G bands. J) Low-magnification TEM image of {W<sub>18</sub>}@SWNT.

The G-band of the SWNT shifted positive by 5.5 and 6.5 cm<sup>-1</sup>, respectively, upon formation of {W<sub>12</sub>}@SWNT and {W<sub>18</sub>}@SWNT hybrid materials, confirming that electrons were donated from the SWNT to the POM guests (Figure 1B).<sup>[20]</sup> The shift of the G-band corresponds to charges of 0.017 and 0.020 hole/C-atom in {W<sub>12</sub>}@SWNT and {W<sub>18</sub>}@SWNT, respectively,<sup>[21]</sup> in reasonable agreement with the microscopically estimated stoichiometries (Figure 1D). Charge neutrality of the host-guest complexes negates the need for additional charge-balancing cations in the POM@SWNT systems, a conclusion supported by the absence of potassium signals from the EDX analysis and X-ray photoelectron spectra of {W<sub>18</sub>}@SWNT (see the Supporting Information).

Solution phase voltammetry of {W<sub>12</sub>} and {W<sub>18</sub>} (Figure 3A–C) is typical of that expected for these materials (see the Supporting Information for details).<sup>[22]</sup> Cyclic voltammograms (CVs) of a POM@SWNT film immobilized on a glassy-carbon electrode (black lines in Figure 3B,C) show that the POMs remain electrochemically active when encapsulated

within the SWNTs. The first two reductions of {W<sub>12</sub>} shift negatively by about 0.2 V upon encapsulation and  $\Delta E_p$  decreases to about 10 mV at a scan rate of 100 mVs<sup>-1</sup> (close to the value of 0 mV expected for a fully electrochemically reversible surface-confined redox couple; Figure S4C,D, Supporting Information).<sup>[23]</sup> Moreover, the peak currents for oxidation/reduction of {W<sub>18</sub>}@SWNT and {W<sub>12</sub>}@SWNT increase linearly as the voltammetric scan rate increases, confirming that the POMs are in intimate contact with the SWNT walls and directly wired to the glassy-carbon current collector (Figure S4A,B, Supporting Information). Integration of the charge under the first reduction waves in the CVs of {W<sub>18</sub>}@SWNT and {W<sub>12</sub>}@SWNT gives surface concentrations,  $\Gamma$ , of 33 and 19 nmol cm<sup>-2</sup>, respectively, indicating that 80–90% of the immobilized POMs are electrochemically addressable.  $\Gamma$  is independent of the scan rate, and  $\Delta E_p$  increases very little as the scan rate increases (Figure S4C,D, Supporting Information), indicating that electron transfer to/from the immobilized POMs is rapid. The charge passed during repeated reduction/oxidation



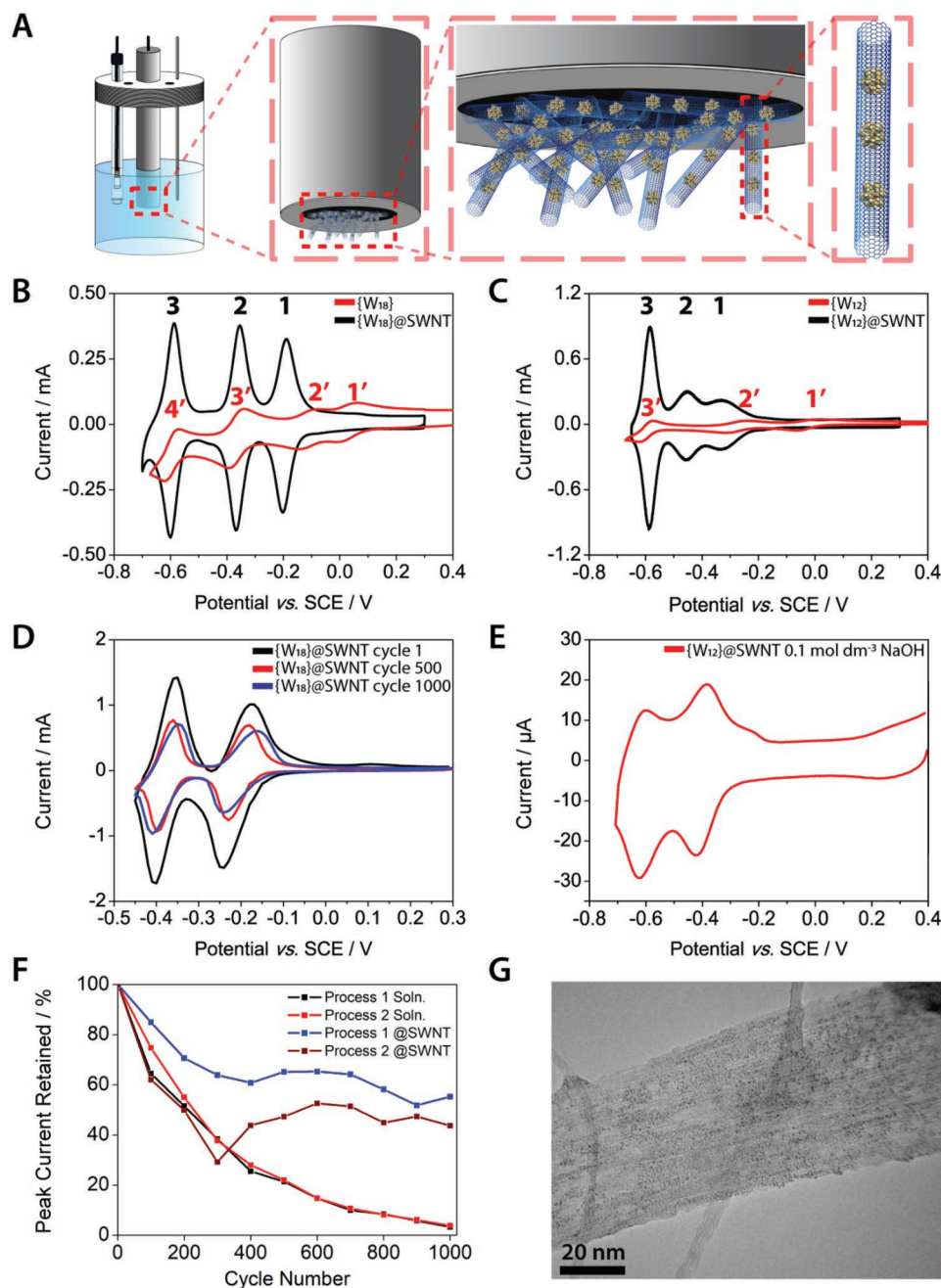


**Figure 3.** A) Schematic of the electrochemical cell used in our study. B,C) Voltammograms of immobilized  $\{W_{18}\}@SWNT$  and  $\{W_{12}\}@SWNT$  films, respectively (black lines). The red lines show voltammograms of  $5.0 \text{ mmol dm}^{-3} K_6\{W_{18}\}$  and  $H_3\{W_{12}\}$ , respectively, recorded using a glassy-carbon working electrode. D) 1st (black), 500th (red), and 1000th (blue) voltammograms of immobilized  $\{W_{18}\}@SWNT$ . All voltammograms were recorded at  $100 \text{ mV s}^{-1}$  in  $1.0 \text{ mol dm}^{-3}$  aqueous  $H_2SO_4$ . E) Voltammogram of immobilized  $\{W_{12}\}@SWNT$  recorded at  $100 \text{ mV s}^{-1}$  in  $0.1 \text{ mol dm}^{-3}$  aqueous NaOH. F) Changes in peak currents for molecules encapsulated inside nanotubes (blue and brown plots) and in solution (red and black plots). The 1st and 2nd reductions of the POMs are referred to as Process 1 and Process 2, respectively. G) TEM image of a large bundle of nanotubes in the  $\{W_{18}\}@SWNT$  sample after 1000 electrochemical cycles.

of  $\{W_{18}\}@SWNT$  remains at 58% of the initial level after 1000 cycles (Figure 3D,F), while free  $\{W_{18}\}$  completely loses activity after 1000 cycles under the same conditions (Figure 3F and Figure S5, Supporting Information). TEM analysis of  $\{W_{18}\}@SWNT$  after CV measurements clearly shows that most POMs remain encapsulated and intact even after 1000 charge–discharge

cycles (Figure 3G). We also tested the (electro)chemical stability of the encapsulated POM@SWNT in aqueous NaOH (pH 13), an environment in which POMs are usually hydrolyzed and decompose readily. TEM analysis shows that the POMs remain intact within the SWNT after contact with the alkaline medium (Figure S6, Supporting Information).

Furthermore, CVs of {W<sub>12</sub>}@SWNT recorded at pH 13 reveal two well-defined, reversible redox couples with  $\Delta E_p = 17$  mV and 0 mV (for the couples near −0.6 and −0.4 V, respectively, Figure 3E). The redox couples remain visible after as many as 15 potential cycles. In contrast, without the protection offered by the SWNTs, free {W<sub>12</sub>} and {W<sub>18</sub>} instantaneously decompose under the same conditions (Figure S7, Supporting Information). Remarkably, the electrochemical signature of POM@SWNT that was eventually lost in alkaline media could be recovered by immersing the POM@SWNTs in an acidic medium (Figure S8, Supporting Information), demonstrating that the POM is protected within the SWNT at pH 13.

In summary, we have discovered an effective method for driving the encapsulation of POMs within SWNTs. The encapsulation process occurs spontaneously and irreversibly at room temperature in water, driven by emergent coulombic forces between the anionic POMs and cationic nanotubes, and yields effectively filled POM@SWNT hybrid materials. The encapsulated POMs retain their redox properties, even in environments in which POMs cannot usually exist. The reagent-free redox-driven nanoconfinement of hydrophilic polyanionic materials within hydrophobic nanoscale carbon channels (which until now were considered incompatible) opens up new opportunities for the scalable and sustainable synthesis of hybrid functional materials from POMs combined with other types of porous carbons and other nanomaterials.

## Supporting Information

Supporting Information is available from the Wiley Online Library or from the author.

## Acknowledgements

J.W.J., G.A.L., D.A.W., G.N.N., and A.N.K. thank the EPSRC for funding through the Centre for Doctoral Training in Sustainable Chemistry (EP/L015633/1). D.A.W. thanks the EPSRC for funding through project EP/P002382/1. U.K. and J.B. thank the DFG and the State Baden Württemberg for financial support in the frame of the SALVE project. A.N.K. thanks the EPSRC (Established Career Fellowship). D.A.W. and G.N.N. thank the Advanced Molecular Materials RPA and Propulsion Futures Beacon of Excellence within the University of Nottingham. The authors thank Dr. Emily Smith and Dr. Jesum Alves Fernandes for assistance with XPS measurements and discussion.

## Conflict of Interest

The authors declare no conflict of interest.

## Keywords

carbon nanotubes, electrochemistry, nanoconfinement, polyoxometalates, redox materials

Received: July 1, 2019  
Revised: August 2, 2019  
Published online: August 26, 2019

- [1] a) B. Dunn, H. Kamath, J.-M. Tarascon, *Science* **2011**, 334, 928; b) Z. Liu, A. A. Yasseri, J. S. Lindsey, D. F. Bocian, *Science* **2003**, 302, 1543; c) D. J. Wales, Q. Cao, K. Kastner, E. Karjalainen, G. N. Newton, V. Sans, *Adv. Mater.* **2018**, 30, 1800159.
- [2] D. L. Long, E. Burkholder, L. Cronin, *Chem. Soc. Rev.* **2007**, 36, 105.
- [3] C. Busche, L. Vilà-Nadal, J. Yan, H. N. Miras, D. L. Long, V. P. Georgiev, A. Asenov, R. H. Pedersen, N. Gadegaard, M. M. Mirza, D. J. Paul, J. M. Poblet, L. Cronin, *Nature* **2014**, 515, 545.
- [4] N. I. Gumerova, A. Rompel, *Nat. Rev. Chem.* **2018**, 2, 0112.
- [5] a) W. Chen, L. Huang, J. Hu, T. Li, F. Jia, Y.-F. Song, *Phys. Chem. Chem. Phys.* **2015**, 16, 19668; b) Y. Ji, L. Huang, J. Hu, C. Streb, Y.-F. Song, *Energy Environ. Sci.* **2015**, 8, 776.
- [6] F. M. Toma, A. Sartorel, M. Iurlo, M. Carraro, P. Parisse, C. Maccato, S. Rapino, B. Rodriguez, Gonzalez, H. Amenitsch, T. Da Ros, L. Casalis, A. Goldoni, M. Marcaccio, G. Scorrano, G. Scoles, F. Paolucci, M. Prato, M. Bonchio, *Nat. Chem.* **2010**, 2, 826.
- [7] D. Ma, L. Liang, W. Chen, H. Liu, Y.-F. Song, *Adv. Funct. Mater.* **2013**, 23, 6100.
- [8] J. Hu, Y. Ji, W. Chen, C. Streb, Y. F. Song, *Energy Environ. Sci.* **2016**, 9, 1095.
- [9] J. Sloan, G. Matthewman, C. Dyer-Smith, A.-Y. Sung, Z. Liu, K. Suenaga, A. I. Kirkland, E. Flahaut, *ACS Nano* **2008**, 2, 966.
- [10] a) J. M. Wynn, P. V. C. Medeiros, A. Vasylenko, J. Sloan, D. Quigley, A. J. Morris, *Phys. Rev. Mater.* **2017**, 1, 073001(R); b) P. V. C. Medeiros, S. Marks, J. M. Wynn, A. Vasylenko, Q. M. Ramasse, D. Quigley, J. Sloan, A. J. Morris, *ACS Nano* **2017**, 11, 6178.
- [11] R. R. Meyer, J. Sloan, R. E. Dunin-Borkowski, A. I. Kirkland, M. C. Novotny, S. R. Bailey, J. L. Hutchison, M. L. H. Green, *Science* **2000**, 289, 1324.
- [12] a) Z. Wang, K. Zhao, H. Li, Z. Liu, Z. Shi, J. Lu, K. Suenaga, S.-K. Joung, T. Okazaki, Z. Jin, Z. Gu, Z. Gao, S. Iijima, *J. Mater. Chem.* **2011**, 21, 171; b) Z. Wang, H. Li, Z. Liu, Z. Shi, J. Lu, K. Suenaga, S.-K. Joung, T. Okazaki, Z. Gu, J. Zhou, Z. Gao, G. Li, S. Sanvito, E. Wang, S. Iijima, *J. Am. Chem. Soc.* **2010**, 132, 13840; c) T. W. Chamberlain, T. Zoberbier, J. Biskupek, A. Botos, U. Kaiser, A. N. Khlobystov, *Chem. Sci.* **2012**, 3, 1919; d) T. Zoberbier, T. W. Chamberlain, J. Biskupek, N. Kuganathan, S. Eyhusen, E. Bichoutskaia, U. Kaiser, A. N. Khlobystov, *J. Am. Chem. Soc.* **2012**, 134, 3073.
- [13] S. T. Skowron, T. W. Chamberlain, J. Biskupek, U. Kaiser, E. Besley, A. N. Khlobystov, *Acc. Chem. Res.* **2017**, 50, 1797.
- [14] D. A. Britz, A. N. Khlobystov, *Chem. Soc. Rev.* **2006**, 35, 637.
- [15] M. T. Pope, G. M. Varga, *Inorg. Chem.* **1966**, 5, 1249.
- [16] A. Botos, J. Biskupek, T. W. Chamberlain, G. A. Rance, C. T. Stoppiello, J. Sloan, Z. Liu, K. Suenaga, U. Kaiser, A. N. Khlobystov, *J. Am. Chem. Soc.* **2016**, 138, 8175.
- [17] A. Al-zubaidi, T. Inoue, T. Matsushita, Y. Ishii, T. Hashimoto, S. Kawasaki, *J. Phys. Chem. C* **2012**, 116, 7681.
- [18] R. L. McSweeney, T. W. Chamberlain, M. Baldoni, M. A. Lebedeva, E. S. Davies, E. Besley, A. N. Khlobystov, *Chem. - Eur. J.* **2016**, 22, 13540.
- [19] N. Vats, S. Rauschenbach, W. Sigle, S. Sen, S. Abb, A. Portz, M. Dürr, M. Burghard, P. A. van Aken, K. Kern, *Nanoscale* **2018**, 10, 4952.
- [20] a) H. Kataura, Y. Kumazawa, Y. Maniwa, I. Umez, S. Suzuki, Y. Ohtsuka, Y. Achiba, *Synth. Met.* **1999**, 103, 2555; b) M. V. Kharlamova, *Prog. Mater. Sci.* **2016**, 77, 125.
- [21] G. U. Sumanaseker, J. L. Allen, S. L. Fang, A. L. Loper, A. M. Rao, P. C. Eklund, *J. Phys. Chem. B* **1999**, 103, 4292.
- [22] M. Sadakane, E. Steckhan, *Chem. Rev.* **1998**, 98, 219.
- [23] A. J. Bard, L. R. Faulkner, *Electrochemical Methods: Fundamental and Applications*, 2nd ed., John Wiley & Sons, New York **2001**, p. 591.